Journal of Peptide Science
J. Peptide Sci. **6**: 26–35 (2000)

Synthesis, Conformational Analysis and Bioactivity of Lan-7, a Lanthionine Analog of TT-232

HAITAO LI[a,1], XIAOHUI JIANG[a,2], STEPHEN B. HOWELL[b] and MURRAY GOODMAN[a,*]

[a] Department of Chemistry and Biochemistry, University of California at San Diego, La Jolla, CA, USA
[b] Cancer Center, University of California at San Diego, La Jolla, CA, USA

Received 14 June 1999
Accepted 26 August 1999

Abstract: A sandostatin analog, TT-232 (D-Phe-c[Cys-Tyr-D-Trp-Lys-Cys]-Thr-NH_2), exhibits strong anti-tumor effects both *in vitro* and *in vivo*. In order to study the structure–activity relationships of TT-232, we designed and synthesized an analog of TT-232, namely Lan-7, in which the disulfide bridge is replaced by a lanthionine monosulfide bridge. Conformational analysis by NMR spectroscopy and computer simulations revealed that Lan-7 and TT-232 adopt very similar conformations in solution, which are quite different from the preferred conformations of sandostatin. Lan-7 has significant growth inhibition effects on a number of human tumor cell lines. It can also induce apoptosis in human ovarian carcinoma 2008 cells. At the same time, Lan-7 produced no toxicity to normal human hematopoietic progenitor cells. All of these results indicate that the modification we made does not alter the anti-tumor activity of TT-232. Copyright © 2000 European Peptide Society and John Wiley & Sons, Ltd.

Keywords: antitumor; apoptosis; conformational analysis; lanthionine; sandostatin

INTRODUCTION

Somatostatin is a tetradecapeptide originally isolated from ovine hypothalamus as a growth hormone (GH) release inhibitor [1]. Many other physiological functions of somatostatin have also been identified, including the inhibition of the release of gastrin, insulin, glucagon and other intestinal hormones, and the suppression of gastric and pancreatic exocrine secretion [2]. Furthermore, somatostatin has anti-proliferative effects and functions as an important hormonal regulator of cell proliferation and differentiation [3].

For therapeutic use, a number of somatostatin analogs, such as Octreotide (Sandostatin) (D-Phe-c[Cys-Phe-D-Trp-Lys-Thr-Cys]-Thr(ol)) [4], Lanreotide (BIM-23014) (D-Nal-c[Cys-Tyr-D-Trp-Lys-Val-Cys]-Thr-NH_2) and Vipreotide (RC-160) (D-Phe-c[Cys-Tyr-D-Trp-Lys-Val-Cys]-Trp-NH_2) [5], have been developed as anti-secretory and anti-proliferative agents. These analogs have increased *in vivo* stability compared with somatostatin and have been used in the clinic for the treatment of acromegaly and hormone-secreting tumors [6]. However, their administration as anti-tumor agents is limited because of side effects [7,8].

In recent years, a sandostatin analog, TT-232 (D-Phe-c[Cys-Tyr-D-Trp-Lys-Cys]-Thr-NH_2), was synthesized by Keri *et al.* [9–11]. This compound exhibits strong anti-tumor effects both *in vitro* and *in vivo*. It can induce apoptosis in a pancreatic tumor cell line, inhibit tyrosine kinase activity and

Abbreviations: DMSO, dimethylsulfoxide; DCM, dichloromethane; FAB-MS, fast atom bombardment mass spectrometry; GH, growth hormone; NMR, nuclear magnetic resonance; ROESY, rotating frame nuclear Overhauser spectroscopy; RP-HPLC, reverse-phase high-performance liquid chromatography; SAR, structure–activity relationships; TLC, thin layer chromatography; TFA, trifluoroacetic acid; TOCSY, total correlation spectroscopy; TPPI, time proportional phase increment.

* Correspondence to: Department of Chemistry and Biochemistry, University of California at San Diego, La Jolla, California 92093-0343, USA.
[1] Agouron Pharmaceuticals Inc., 3550 General Atomics Court, San Diego, CA 92121, USA.
[2] Molecular Simulations Inc., 9685 Scranton Road, San Diego, CA 92121, USA.

CCC 1075–2617/2000/0100026-10$17.50

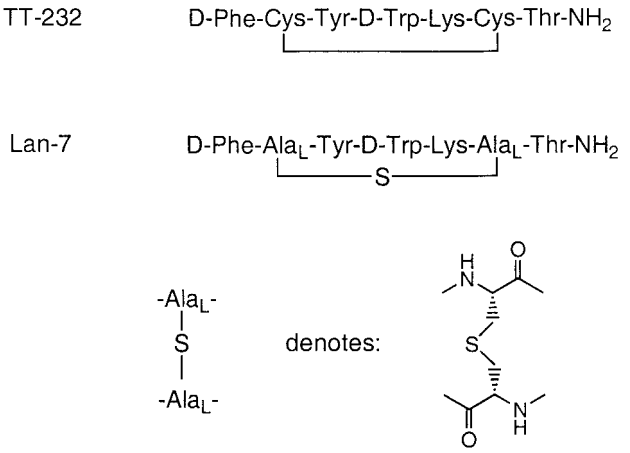

Figure 1 The structures of TT-232 and its lanthionine analog Lan-7.

stimulate tyrosine phosphatase activity in colon tumor cell lines. Although TT-232 was derived as a somatostatin analog, it does not inhibit GH release. This selectivity is believed to relate to its unique backbone structure that has five residues within the disulfide ring in place of six residues in sandostatin-like analogs.

The structure–activity relationship (SAR) for TT-232 has not been elucidated. The five-residue cyclic structure and the specific amino acid sequence are apparently important for its unique activity. Jaspers *et al.* [12] carried out NMR studies of TT-232 in CD_3OH at 243 K. They showed that the backbone of TT-232 behaves differently from sandostatin analogs. The typical type II′ β turn around D-Trp-Lys no longer exists in TT-232.

In order to extend the study of SAR of TT-232, we designed and synthesized an analog of TT-232 in which the disulfide bridge is replaced by a lanthionine monosulfide bridge (Figure 1). This modification is designed to reduce both the size and the flexibility of the five-residue ring structure, and to increase its enzymatic stability. This new analog, denoted Lan-7, was tested for anti-tumor-related activities. In addition, conformational analyses of Lan-7 and TT-232 were carried out by NMR and computer simulations to elucidate the SAR.

MATERIALS AND METHODS

General

The protected amino acids were purchased from either Bachem Bioscience (Torrance, CA) or Novabiochem (San Diego, CA). The reagents EDC [*N*-ethyl-*N*′-(3-dimethylamino propyl)carbodiimide] and BOP [benzotriazol-1-yloxy-tris(dimethylamino)-phosphonium hexafluorophosphate] were purchased from Chem-Impex International (Wood Dale, IL), and HBTU [*O*-(benzotriazol-1-yl)-*N*,*N*,*N*′,*N*′-tetramethyluronium hexafluorophosphate] from Applied Biosystem (Foster City, CA). The new coupling reagent, 3-(diethoxyphosphoryloxy)-1,2,3-benzotrazin-4(3H)-one (DEPBT) [13], was a kind gift from Professor Y.H. Ye in Peking University, China. Mass spectra were obtained from Scripps Research Institute. Thin layer chromatography (TLC) was carried out on silica gel 60 (F_{254}) plates.

Boc-Cys-Thr(Bzl)-NHCHPh$_2$ 1

To Boc-Cys(ACM)-Thr(Bzl)-NHCHPh$_2$ (3.64 g, 5.6 mmol) in 32 ml glacial acetic acid and 8 ml water was added $Hg(OAc)_2$ (4.47 g, 11.2 mmol). After stirring at room temperature (r.t.) for 3 h, H_2S was bubbled through the solution for 1 h. Black precipitate immediately appeared. The reaction mixture was filtered through celite pad. The filtrate was evaporated to dryness. Flash chromatography (EtOAc:hexanes = 1:1) afforded the desired product **1** as a white powder (2.26 g, 70%). $R_F = 0.56$ (EtOAc: hexanes = 1:1). FAB-MS m/z 578 $(M+H)^+$, 600 $(M+Na)^+$, 616 $(M+K)^+$. ^{1}H-NMR (360 MHz, $CDCl_3$) δ 0.95 (d, $J = 6$ Hz, 3H from Thr), 1.13 (s, 9H, Boc), 2.75 (m, 2H, β of Cys), 3.90–4.00 (m, 6H, α of Cys and α of Thr, β of Thr, methylene from Bzl, -CH- from amide protection), 5.12 (br, 1H, amide), 6.05 (br, 1H, amide), 6.66–7.18 (m, 16H, aromatics and one amide).

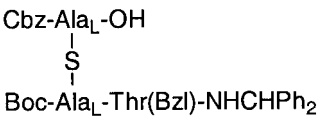

2

To Boc-Cys-Thr(Bzl)-NHCHPh$_2$ **1** (1.36 g, 2.36 mmol) in DMF (16 ml) was added Cbz-Ser-β-lactone (1.56 g, 7.05 mmol) and Cs_2CO_3 (0.392 g, 1.18 mmol). The reaction was stirred at r.t. for 5 h. The solvent was removed under reduced pressure. The crude product was dissolved in EtOAc (250 ml), washed with brine (3 × 10 ml), 5% $NaHSO_4$ (3 × 10 ml), dried over Na_2SO_4, and evaporated to dryness. Column chromatography ($CHCl_3$:MeOH = 90:10) afforded the desired tripeptide lanthionine **2** as a white foam (658 mg, 35%). $R_F = 0.58$ ($CHCl_3$:MeOH:NH_4OH = 75:25:5). Electrospray MS m/z 799 $(M+H)^+$, 821 $(M+Na)^+$, 837 $(M+K)^+$. ^{1}H-NMR (360 MHz, $CDCl_3$) δ 1.08 (d, $J = 6$ Hz, 3H

from Thr), 1.27 (s, 9H, Boc), 2.82 (m, 4H, β of lanthionine), 3.89–4.72 (m, 7H, 2α of lanthionine, 1α of Thr, β of Thr, methylene from BzL, -CH- from amide protection), 5.00 (s, 2H, methylene from Cbz), 5.63 (br, 1H, amide), 6.18 (br, 1H, amide), 7.15 (br, 20H, aromatics and amides), 7.66 (br, 1H, amide).

Cbz-D-Phe-Ala$_L$-OH
S
Boc-Ala$_L$-Thr(Bzl)-NHCHPh$_2$ **3**

To the tripeptide lanthionine **2** (661 mg, 0.83 mmol) was added acetic acid (6.5 ml). The solution was degassed before the addition of 30% Pd/C (1.3 g) and 1,4-cyclohexadiene (1.54 ml, 16.6 mmol). After stirring at r.t. overnight, another batch of 1,4-cyclohexadiene (1.54 ml, 16.6 mmol) was added. After successive addition of another two batches of 1,4-cyclohexadiene (1.54 ml $\times$ 2), the reaction mixture was filtered through celite. The crude product was dissolved in EtOAc (250 ml), washed with brine (3 $\times$ 2 ml), 5% $NaHCO_3$ (3 $\times$ 2 ml), dried over Na_2SO_4, and evaporated to dryness. To this deprotected material in THF (5 ml) was added Cbz-D-Phe-NCA (296 mg, 0.91 mmol) and 4-EM (10.5 µl, 0.083 mmol). The reaction was stirred at r.t. overnight. The solvent was removed under reduced pressure. Column chromatography ($CHCl_3$:MeOH = 90:12) afforded the desired tetrapeptide lanthionine **3** as a white foam (260 mg, 50%). $R_F = 0.60$ ($CHCl_3$:MeOH:NH_4OH = 75:25:5). Electrospray MS m/z 946 $(M + H)^+$, 968 $(M + Na)^+$, 984 $(M + K)^+$. ^{1}H-NMR (360 MHz, $CDCl_3$) δ 1.08 (d, J = 6Hz, 3H from Thr), 1.27 (s, 9H, Boc), 2.82 (m, 4H, β of lanthionine), 3.89–4.72 (m, 7H, 2α of lanthionine, 1α of Thr, β of Thr, methylene from Bzl, -CH- from amide protection), 5.00 (s, 2H, methylene from Cbz), 5.63 (br, 1H, amide), 6.18 (br, 1H, amide), 7.15 (br, 20H, aromatics and amides), 7.66 (br, 1H, amide).

Cbz-D-Phe-Ala$_L$-Tyr(ZBr)-D-Trp-Lys(ZCl)-OPac
S
Boc-Ala$_L$-Thr(Bzl)-NHCHPh$_2$ **4**

To a solution of Boc-Tyr(ZBr)-D-Trp-Lys(ZCl)-OPac (347 mg, 0.317 mmol) in DCM (2 ml) was added TFA (2 ml). The resulting solution was stirred at r.t. for 30 min. The solvent was removed under reduced pressure. The product was obtained as a light yellow foam. It was used directly in the next step. To a solution of the deprotected material (250 mg, 0.264 mmol), HOBt (44.5 mg, 0.29 mmol) and 4-EM (67 µl, 0.528 mmol) in DMF (5 ml) was added EDC (6.08 mg, 0.317 mmol). The solution was stirred at 0°C for 30 min and gradually warmed to r.t. and stirred for 18 h. The crude product was dissolved in $CDCl_3$ (60 ml), washed with 5% $NaHCO_3$ (3 $\times$ 1 ml), brine (3 $\times$ 1 ml), 5% $NaHSO_4$ (3 $\times$ 1 ml), dried over Na_2SO_4, and evaporated to dryness. Column chromatography ($CHCl_3$:MeOH = 90:10) afforded the desire product **4** as a white foam (394 mg, 77.5%). $R_F = 0.27$ ($CHCl_3$:MeOH:HOAc = 100:5:1). Electrospray MS m/z 1924 $(M + H)^+$, 1946 $(M + Na)^+$.

Cbz-D-Phe-Ala$_L$-Tyr(ZBr)-D-Trp-Lys(ZCl)-Ala$_L$-Thr(Bzl)-NHCHPh$_2$
S **5**

Removal of phenacyl ester. Activated zinc dust (1 g) was added to a solution of compound **4** (379 mg, 0.197 mmol) in glacial acetic acid (10 ml). The suspension was stirred at r.t. for 15 h. The mixture was filtered to remove the insoluble metal compounds. The filtrate was evaporated to dryness. Column chromatography ($CHCl_3$:MeOH = 90:10) afforded the desired acid. $R_F = 0.31$ ($CHCl_3$:MeOH:HOAc = 100:5:1). Electrospray MS m/z 1806 $(M + H)^+$, 1828 $(M + Na)^+$.

Removal of Boc. To the acid obtained above (332 mg, 0.184 mmol) in DCM (2.5 ml) was added TFA (2.5 ml). After stirring at r.t. for 1 h, the solvent was removed under reduced pressure. No further purification was carried out; the product was directly used in the next step. $R_F = 0.15$ ($CHCl_3$:MeOH:HOAc = 100:5:1).

Cyclization. To the above deprotected material in DMF (120 ml) at 4°C was added 4-EM (72 µl, 0.54 mmol) and DEPBT (220 mg, 0.72 mmol). After stirring at r.t. for 48 h, the solvent was removed under reduced pressure. The desired cyclic product **12** was precipitated out by addition of diethyl ether (214 mg, 70%). $R_F = 0.4$ ($CHCl_3$:MeOH:HOAc = 100:5:1). Because the product had very bad solubility in all common solvents, it was deprotected and characterized after the final deprotection.

D-Phe-Ala$_L$-Tyr-D-Trp-Lys-Ala$_L$-Thr-NH_2 **6**
S

The fully protected peptide (107 mg, 0.063 mmol) was treated with HF/anisole (5 ml/0.5 ml) at -10°C for 30 min and at 0°C for 30 min. Diethylether was added to precipitate out the deprotected peptide. Purification of the final product was carried out on RP-HPLC (gradient: 10–50% CH_3CN/H_2O with 0.1% TFA over 30 min; flow rate: 4 ml/min). Compound

13 was obtained as a white powder (45 mg, 77%). Electrospray MS m/z 915 $(M+H)^+$, 937 $(M+Na)^+$. FT-MALDI-MS m/z expected 915.4187 $(M+H)^+$, found 915.4189.

D-Phe-c(Cys-Tyr-D-Trp-Lys-Cys)-Thr-NH_2 TT232

Peptide synthesis. Peptide synthesis was carried out on an ABD 433A synthesizer using Fmoc chemistry and HBTU activation. The scale of the synthesis was 0.1 mmol. The substitution level of the Rink Amide MBHA resin was 0.49 mmol; therefore, 204 mg resin was used. The synthesis started with the deprotection of the resin with piperidine, followed by coupling of the first amino acid Fmoc-Thr(*t*Bu)-OH (397 mg, 1 mmol) with HBTU. After successive coupling of Fmoc-Cys(Acm)-OH (414 mg, 1 mmol), Fmoc-Lys-(Boc)-OH (468 mg, 1 mmol), Fmoc-D-Trp-OH (526 mg, 1 mmol), Fmoc-Tyr(*t*Bu)-OH (459 mg, 1 mmol), Fmoc-Cys(Acm)-OH (414 mg, 1 mmol) to the resin, Boc-D-Phe-OH (265 mg, 1 mmol) was coupled as the last residue.

Disulfide formation. The peptide bound resin was transferred to a small reaction vessel and treated with I_2 (0.25 g, 1 mmol) in DMF (10 ml) for 1 h. The resin was thoroughly washed with DMF and DCM and dried under high vacuum.

Cleavage. The peptide-bound resin was treated with cleavage mixture (9.5 ml TFA, 0.25 ml anisole and 0.25 ml water) for 1 h. The reaction mixture was flittered and the filtrate was taken to dryness. The crude material was dissolved in water (60 ml) and extracted with diethyl ether. The water layer was lyophilized and the crude product was purified by RP-HPLC (conditions: 18% CH_3CN/H_2O with 0.1%; flow rate: 8 mL/min). **TT-232** was obtained as a white powder (30 mg, 31%). FAB-MS m/z 947 $(M+H)^+$.

Biological Assays

The effects of Lan-7 and TT-232 on human malignant cell lines, the cytotoxicity of Lan-7 to normal human hematopoietic progenitor cells, and the ability of Lan-7 to induce apoptosis in 2008 cell line were studied using previously published procedures [14]. The binding affinities of Lan-7 and TT-232 to cloned somatostatin receptors were determined using a published protocol [15,16].

NMR Experiments

The samples were dissolved in DMSO-d_6 at concentrations of approximately 3–6 mM. The ^{1}H-NMR spectra were measured on a Bruker AMX 500 spectrometer operating at 500 MHz. The one-dimensional (1D) spectra contain 16384 data points with a spectral width of 6000–6500 Hz. The 1D spectra, acquired at temperatures of between 300 and 320 K, were used to measure the amide proton temperature coefficients. The two-dimensional (2D) spectra were acquired at 300 K for assignments and NOE measurements, and 300–320 K for the total correlation spectroscopy (TOCSY) to measure the amide proton temperature coefficients that are overlapped in the 1D spectra. The TOCSY experiments were performed using the MLEV-17 sequence and the time proportional phase increment (TPPI). A mixing time of 75 ms with a spin-locking field of 10 kHz was employed. The rotating frame nuclear Overhauser spectroscopy (ROESY) experiments were carried out with a mixing time of around 150 ms. A spin-locking field of 2.5 kHz was used. The TOCSY and ROESY experiments were obtained using 2000 data points in the $f2$ domain and 256–512 data points in the $f1$ domain.

The spectra were processed using the program FELIX (Molecular Simulations Inc., San Diego). Zero filling was applied in the $f1$ and $f2$ domains to obtain a matrix of $2k \times 2k$ data points. Multiplication with a phase-shifted sine-bell function was employed to enhance the spectra. Chemical shifts were measured using DMSO-d_6 ($\delta = 2.49$ ppm) as an internal standard.

Computer Simulations

The distance geometry program DGEOM was used to generate structures consistent with the distance constraints derived from NOEs. A family of 500 initial conformations was generated. Energy minimization was carried out to remove bad contacts among the atoms. The forcefield CFF91 was employed. A distance dependent dielectric constant (4*r) was used to simulate the solvent effects. The steepest descents algorithm, followed by the quasi-Newton-Raphson algorithm (BFGS) was used for minimization until the maximum derivative was less than 0.01 kcal/mol·Å.

Cluster analysis was performed to divide the conformers into groups according to their backbone torsion angles. Depending on the criteria, usually 10–20 groups were obtained. The lowest energy conformation of each group was used for further studies.

The distance constraints and ϕ angles derived from NMR measurements were compared with the

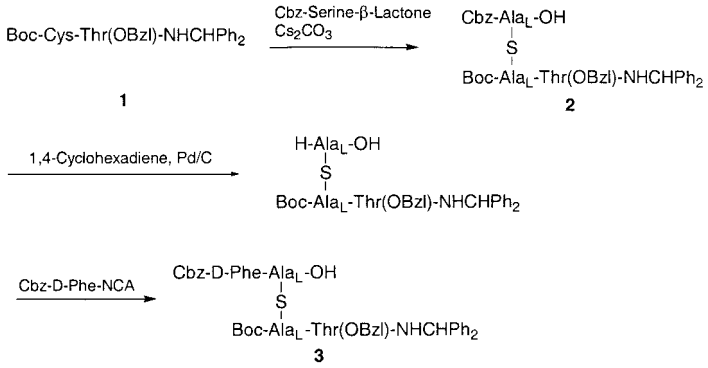

Figure 2 Synthesis of tetrapeptide lanthionine building block.

structures after cluster analysis. An error of $\pm 30°$ was tolerated for the ϕ angles. The structures that violated the above criteria were discarded.

Restrained molecular dynamics was carried out on the structure with the lowest energy and consistent with the NMR data to investigate its dynamic properties. The distance constraints derived from NOEs were applied during the simulations. A quadratic force constant of 25 kcal/mol·Å^2 was employed. The simulations were performed at 298 K for 100 ps with the time step of 1 fs. Trajectories were collected every 1 ps for analysis.

RESULTS AND DISCUSSIONS

Design and Synthesis

Lanthionine is an unusual amino acid composed of two alanine-like residues bridged by a thioether linkage. This cystine mimetic is an important building block of a family of bioactive peptides called lantibiotics [17]. Lanthionine-containing peptides have more constrained structures and are much more stable towards enzymatic degradations as compared with their disulfide counterparts [18]. In the design of the lanthionine TT-232 analog, our strategy focused on constraining the backbone conformation of the biological active TT-232 without changing the spatial arrangements of the side chain functional groups.

In our synthetic strategy, a convergent route was planned in which the protected tetrapeptide lanthionine building block **3** (Figure 2) and the protected tripeptide (Tyr-D-Trp-Lys) were coupled and cyclized to afford the desired product (Figure 3). In this route, the tetrapeptide lanthionine building block was the key intermediate.

In our laboratories, we have developed a synthetic route to prepare orthogonally-protected dipeptide lanthionine building blocks, which involves a regioselective ring opening of *N*-protected serine β-lactone with a sulfhydryl group from a protected cysteine derivative [19]. Following the same rationale, we hoped to have Cbz-D-Phe-Ser-β-lactone react with sulfhydryl from Boc-Cys-Thr(Bzl)-NHCHPh$_2$, which would directly lead to the tetrapeptide lanthionine. Unfortunately, the Mitsunubu reaction on Cbz-D-Phe-Ser-OH gave the dipeptide β-lactone in an extremely low yield (10%). This forced us to develop another synthetic route, which involved the ring opening of Cbz-Ser-β-lactone by Boc-Cys-Thr(Bzl)-NHCHPh$_2$ to prepare the tripeptide lanthionine, followed by coupling of Cbz-D-Phe-OH to the tripeptide in order to obtain the desired tetrapeptide lanthionine derivative (Figure 2). This reaction sequence proceeded smoothly with reasonable yields.

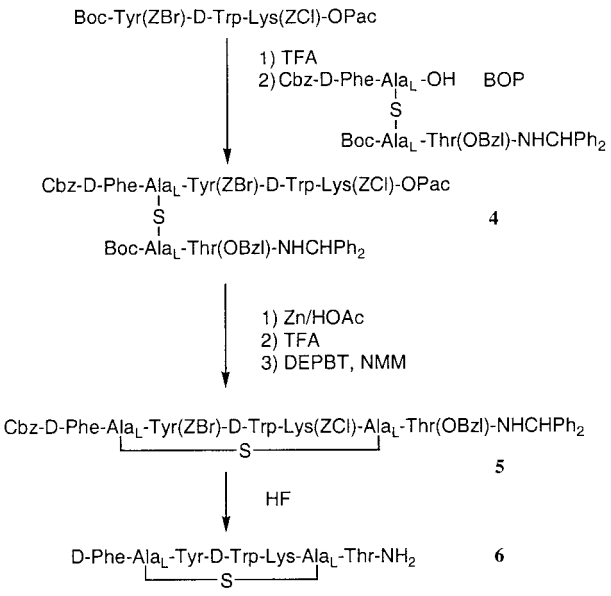

Figure 3 Synthesis of Lan-7 in solution.

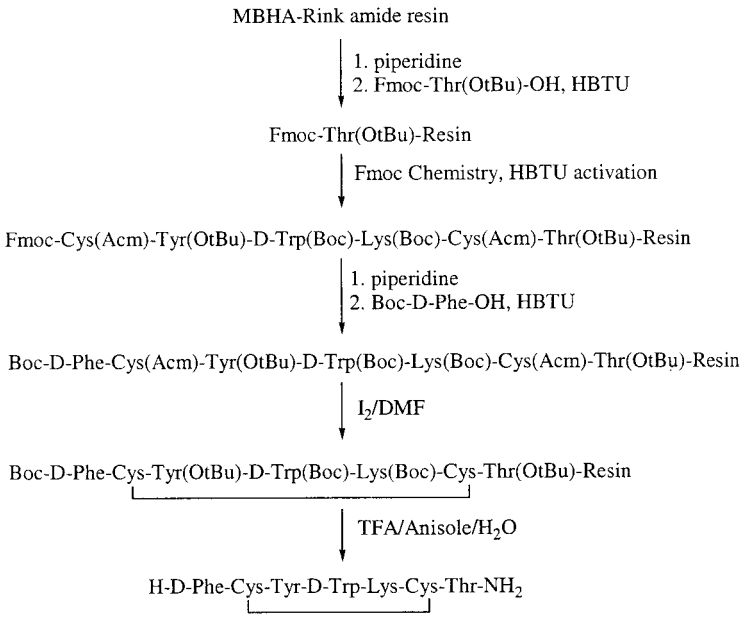

Figure 4 Solid phase synthesis of TT-232.

The tripeptide, Boc-Tyr(ZBr)-D-Trp-Lys(ZCl)-OPac, was synthesized using Boc chemistry and the EDC/HOBT activation method. It was coupled to the lanthionine building block **3** to afford the linear heptapeptide (Figure 3). After removal of the phenacyl ester (-*O*Pac) from the *C*-terminus and Boc from *N*-terminus, the linear peptide was cyclized by a new coupling reagent, 3-(diethoxyphosphoryloxy)-1,2,3-benzotrazin-4(3H)-one (DEPBT) [13], to afford the fully protected heptapeptide **5**. Treatment with hydrogen fluoride removed all the protecting groups to yield Lan-7.

The parent compound TT-232 was assembled on a solid support using standard solid phase peptide synthesis procedure (Figure 4) involving Fmoc chemistry and HBTU activation. A Rink amide MBHA resin was used as the solid support. After formation of the disulfide bridge by iodine oxidation on the resin, the peptide was cleaved from the resin by TFA with simultaneous removal of the protecting groups.

Lan-7 and TT-232 were purified by RP-HPLC. FAB and electrospray mass spectrometries were used to verify the identities of all intermediates and final products. The structural details of each compound were investigated by 1D and 2D ^{1}H-NMR spectroscopy. In addition, high-resolution mass spectrometry and analytical HPLC were used to characterize the final products.

Biological Results

The anti-tumor activities of Lan-7, together with TT-232 and sandostatin, were studied in several human malignant cell lines. It was shown that Lan-7 and TT-232 have the same dose range to inhibit the proliferation of tumor cell lines, which is about two to three times more potent than sandostatin (Table 1) [14].

Because a high degree of selectivity for the effects on tumor cells is an essential requirement for an anti-cancer agent, the cytotoxicity of Lan-7 to human hematopoeitic precursors was assessed. At concentrations that were highly cytotoxic to human tumor

Table 1 Relative Cytotoxicity (IC_{50} μM) of Lan-7, TT232 and Sandostatin on Human Malignant Cell Lines

Cell lines	Lan-7	TT-232	Sandostatin
2008[a]	16.93±1.84	17.89±1.15	45.04±3.64
UMSCC10b[a]	27.69±2.17	25.24±1.19	82.23±0.26
HCT116[b]	29.97±1.19	28.02±1.17	55.76±6.26
HEC59[b]	36.81±0.40	27.03±2.17	n.d.

[a] Exposure time 48 h.
[b] Exposure time 72 h.
n.d.: Not determined.

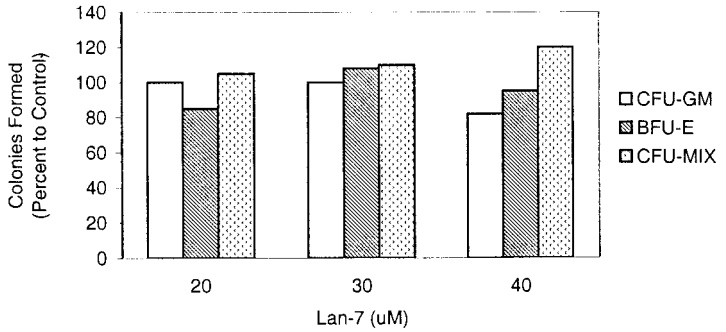

Figure 5 Cytotoxicity of Lan-7 to normal human hematopoietic progenitor cells.

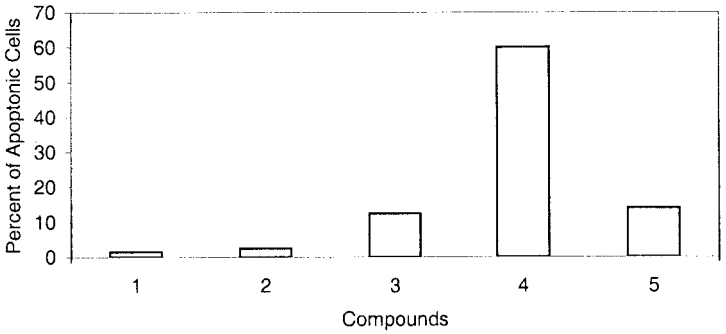

Figure 6 Induction of apoptosis by Lan-7 in 2008 cell line. Compound **1**: negative control; **2**: Lan-7 (10 μM); **3**: Lan-7 (30 μM); **4**: Lan-7 (40 μM); **5**: retinoic acid (RA) (10 μM) + cisplatin (DDP) (40 μM) as positive control.

Table 2 The Binding Affinities (IC_{50}, nM) of Lan-7 and TT-232 to Cloned Somatostatin Receptors

	msst1	msst2b	msst3	msst4	hsst5	rsst5
Lan-7	>1000	>1000	>1000	>1000	>1000	>1000
TT-232	713	>1000	>1000	>1000	565	248

cell lines, Lan-7 produced no significant toxicity to normal human hematopoietic progenitor cells (Figure 5). It was also demonstrated that Lan-7 induced apoptosis in human ovarian carcinoma 2008 cells over the same concentration range at which it produces cytotoxicity (Figure 6).

Because Lan-7 and TT-232 are analogs developed from the structure of somatostatin, their binding affinities of cloned somatostatin receptors (sst1-5) were measured and are shown in Table 2. Both Lan-7 and TT-232 have very low affinities to somatostatin receptors. It was also found from *in vivo* studies that Lan-7 does not inhibit GH release.

NMR Studies

The assignments of proton resonance for Lan-7 and TT-232 in DMSO-d_6 at 300 K are shown in Table 3. The intensities of ROESY cross peaks (Table 4) were calibrated against the cross peak of the H_β protons in Phe, Tyr or D-Trp and were qualitatively classified as strong (s), medium (m) or weak (w). The interproton distance was assigned as 2.5 Å or less for a strong NOE, 2.5–3.0 Å for a medium NOE and 3.0–4.0 Å for a weak NOE. The $J_{NH\text{-}H\alpha}$ coupling constants of Lan-7 and TT-232 were used to calculate the ϕ angles; the results are listed in Table 5. The temperature coefficients of the amide protons of Lan-7 and TT-232 were

measured from 300 to 320 K and are given in Table 6.

The overall chemical shifts of Lan-7 are very similar to those of TT-232, which indicates they have very similar conformations in solution. The main differences arise from the disulfide/monosulfide region. The chemical shifts of β methylenes of residue **2** and **7** are quite different in TT-232 and Lan-7 because of the different ring structures. All the $J_{NH\text{-}H\alpha}$ coupling constants in Lan-7 and TT-232 are above 7. This observation suggests that TT-232 and Lan-7 have extended β structures, which is consistent with the NOE patterns. The NOEs between NH and Hα in the same residue are in the medium range, indicating a

Table 3 The ^{1}H Chemical Shifts of TT-232 and Lan-7

Residue	(δ ppm)	TT-232	Lan-7
D-Phe^1	α	4.11	4.21
	β	3.13, 2.87	3.01, 2.90
	Others	7.30, 7.26, 7.15	7.30, 7.25, 7.12
Cys^2/Ala^2_L	NH	8.70	8.55
	α	4.53	4.59
	β	3.06, 2.75	2.75, 2.52
Tyr^3	NH	8.60	8.50
	α	4.50	4.69
	β	2.79, 2.58	2.65, 2.50
	OH	9.18	9.18
	Others	6.87, 6.55	6.90, 6.58
D-Trp^4	NH	8.12	8.61
	α	4.59	4.3
	β	3.01, 2.85	3.07, 2.81
	Others	10.81, 7.18	10.80, 7.17
		7.53, 6.97	7.54, 6.97
		7.05, 7.30	7.05, 7.30
Lys^5	NH	8.29	8.32
	α	4.05	4.1
	β	1.56, 1.27	1.56, 1.32
	γ, δ	1.04, 1.41	0.96, 1.38
	ε	2.97	2.65
Cys^6/Ala^6_L	NH	8.34	7.99
	α	4.53	4.3
	β	3.09, 2.84	2.72, 2.66
Thr^7	NH	7.40	7.56
	α	4.06	4.1
	β	4.02	3.99
	γ	0.98	0.99
	OH	4.94	4.83

Table 4 The Important NOEs of TT-232 and Lan-7

NOEs	TT-232	Lan-7
D-Phe^1 NH-D-Phe^1 Hα	m	m
Cys^2 NH-D-Phe^1 Hα	s	s
Cys^2 NH-Cys^2 Hα	m	m
Tyr^3 NH–Cys^2 Hα	s	s
Tyr^3 NH–Tyr^3 Hα	m	m
D-Trp^4 NH–Tyr^3 Hα	s	s
D-Trp^4 NH–D-Trp^4 Hα	m	m
Lys^5 NH–D-Trp^4 Hα	s	s
Lys^5 NH–Lys^5 Hα	m	m
Cys^6 NH–Lys^5 Hα	s	s
Cys^6 NH–Cys^6 Hα	m	m
Thr^7 NH–Cys^6 Hα	s	s
Thr^7 NH–Thr^7 Hα	m	m

Cys^2 and Cys^6 are in TT-232. The corresponding residues in Lan-7 are the lanthionine building block. The intensities of NOE signals are classified as strong (s), medium (m) or weak (w).

Table 5 The Coupling Constants $J_{NH\text{-}\alpha}$ and Calculated ϕ of TT-232 and Lan-7

Residue	TT-232		Lan-7	
	$J_{NH\text{-}\alpha}$ (Hz)	Calculated ϕ (deg)	$J_{NH\text{-}\alpha}$ (Hz)	Calculated ϕ (deg)
Cys^2/Ala^2_L	8.8	−99, −140	8.0	−90, −149
Tyr^3	8.4	−95, −144	8.9	−100, −139
D-Trp^4	8.0	90, 149	7.3	84, 155
Lys^5	7.3	−84, −155	8.0	−91, −148
Cys^6/Ala^6_L	7.7	−87, −152	8.0	−91, −148
Thr^7	8.8	−99, −140	8.2	−92, −147

Table 6 The Temperature Coefficients (−ppb/K) of the Amide Protons of TT-232 and Lan-7 in DMSO-d_6

Residue	TT-232	Lan-7
Cys^2/Ala^2_L	5.3	4.3
Tyr^3	5.3	5.0
D-Trp^4	3.5	7.4
Lys^5	7.0	4.2
Cys^6/Ala^6_L	4.1	2.5
Thr^7	2.6	3.9

Table 7 The Torsion Angles for the Cyclic Portion of TT-232 and Lan-7

		Cys^2/Ala^2_L	Tyr^3	D-Trp^4	Lys^5	Cys^6/Ala^6_L
Lan-7	ϕ	−143	−82	136	−154	−84
	ψ	−83	−80	65	−70	−73
	ω	172	−170	−179	−180	−177
	κ_1	−67				−77
	κ_2	167				64
TT-232	ϕ	−136	−122	153	−153	−74
	ψ	−100	−84	64	−93	−60
	ω	169	−172	−179	169	−186
	κ_1	−70				−72
	κ_2	−70				158

distance of 2.5–3.0 Å, while the NOEs of αH and NH between residues i and $i+1$ are very strong with a distance of less than 2.5 Å. This distance pattern is typical for extended β structures. The temperature coefficients of amide protons are relatively high, which suggests that no hydrogen bonds exist in Lan-7 and TT-232.

From NMR studies, it is shown that Lan-7 and TT-232 adopt extended β structures in solution. Because D-Trp^4 is in the middle of the sequence, its inverted chirality changes the direction of the backbone that is cyclized by the lanthionine building block in Lan-7 or by the disulfide between Cys^2 and Cys^6 in TT-232. It is also clear that the β turn about D-Trp-Lys that is characteristic in somatostatin analogs does not exist in Lan-7 and TT-232. This may explain why Lan-7 and TT-232 do not bind to somatostatin receptors.

Computer Simulations

Distance constraints derived from NOE intensity were employed in distance geometry to generate conformations of Lan-7 and TT-232. Cluster analysis and energy minimization were used to select conformers that are consistent with NMR results. The torsional angles of selected conformers of Lan-7 and TT-232 are listed in Table 7. As shown in Plate 1, the selected conformations of Lan-7 and TT-232 share the same backbone structure and the spatial arrangements of side chains. It is also shown that no secondary structures exist in the molecules. Because no NMR constraints involve side chain functional groups, molecular dynamics (MD) were carried out using distance constraints obtained from NMR measurements to simulate the dynamic properties of Lan-7 and TT-232, and to access the side chain flexibility. The MD trajectories of Lan-7 and TT-232 (every 10 ps over 100 ps) are shown in Plate 2. The backbones of Lan-7 and TT-232 are fairly constrained while their side chains are highly flexible. When the two molecules are compared, the ring structure of Lan-7, especially at the monosulfide region, is much more rigid than that of TT-232.

CONCLUSIONS

We designed and synthesized a peptidomimetic analog of TT-232 in which the ring size was reduced by elimination of one sulfur atom from the disulfide bridge. The new analog (Lan-7) exhibits the same anti-tumor activity as TT-232 in the tumor cell lines tested. It was also observed that Lan-7 can induce apoptosis in human ovarian cells. In addition, it was found that Lan-7 does not produce cytotoxicity to human hematopoietic progenitor cells. All of these results indicate that the modification we made does not alter the anti-tumor activity of TT-232. Furthermore, because of its peptidomimetic nature, Lan-7 has therapeutic potential as an anti-cancer agent.

In SAR studies, we determined the conformations of Lan-7 and TT-232 in solution using NMR spectroscopy and computer simulations. It was revealed that Lan-7 and TT-232 adopt very similar conformations. Both molecules have well-defined backbone conformations and the same spatial placements of side chain functional groups. This is consistent with the observation that Lan-7 and TT-232 exhibit the same anti-proliferative activities. On the other hand, because the type II′ β turn does not exist in both molecules, they do not have somatostatin activities. The effect of reduction of ring size in Lan-7 was observed in MD simulations. The cyclic structure in Lan-7 is much more constrained and less flexible, especially in the lanthionine region, as compared

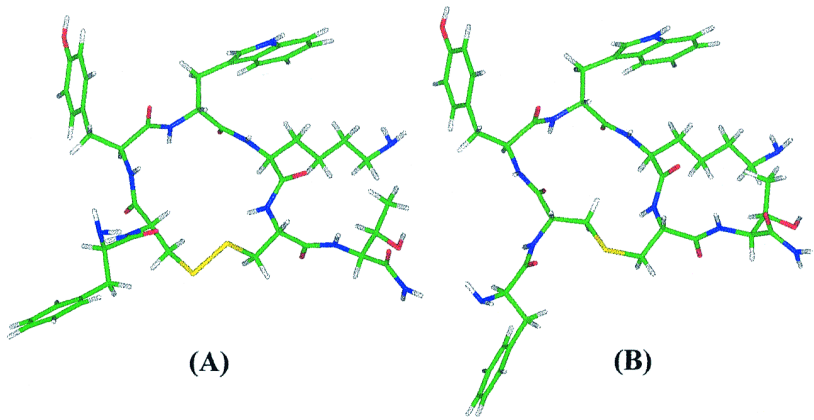

Plate 1 The preferred conformations of TT-232 (A) and Lan-7 (B) in solution determined by NMR and computer simulations.

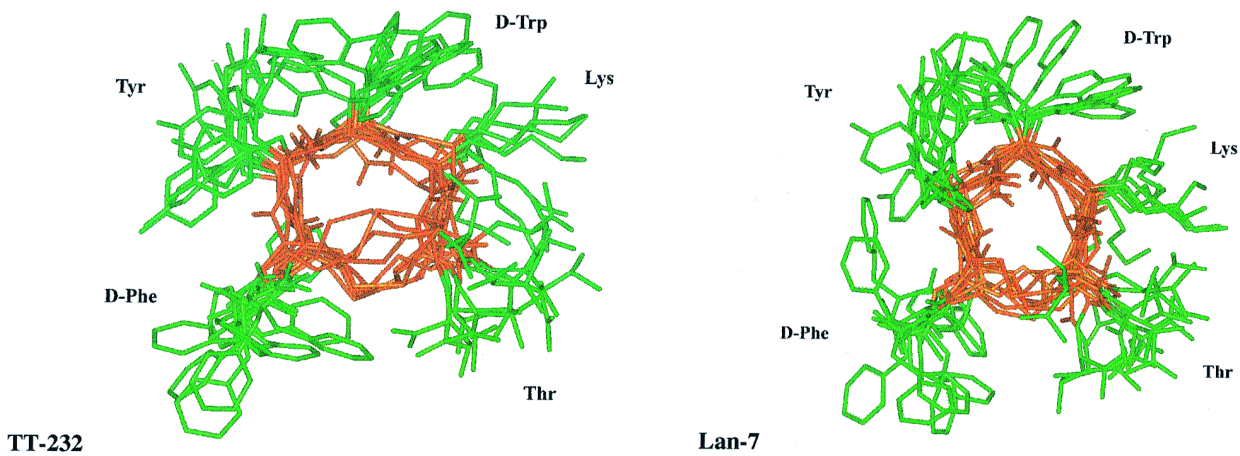

Plate 2 The trajectories (every 10 ps) from constrained molecular dynamics simulations (100 ps) of TT-232 and Lan-7.

with TT-232. Based on these findings, we propose that the anti-tumor activities of Lan-7 and TT-232 come from the spatial arrangements of the side chain functional groups. This model can be used to design non-peptide analogs of TT-232, which may have enhanced enzymatic stability and anti-tumor potency.

Acknowledgements

This research was supported by the National Institute of Health (DK 15410) and the Cancer Center, University of California, San Diego. We would like to thank Dr Hua Zheng at the Cancer Center, University of California, San Diego, and Dr Terry Reisine for biological assays.

REFERENCES

1. Brazeau P, Vale W, Burgus R, Ling N, Butcher M, Rivier J, Guillemin R. Hypothalamic polypeptide that inhibits the secretion of immunoreactive pituitary growth hormone. *Science* 1973; **179**: 77–79.
2. Reichlin S. Somatostatin. *New Engl. J. Med.* 1983; **309**: 1495–1501.
3. Lamberts SW, Krenning EP, Reubi JC. The role of somatostatin and its analogs in the diagnosis and treatment of tumors. *Endocrine Rev.* 1991; **12**: 450–482.
4. Bauer W, Briner U, Doepfner W, Haller R, Huguenin R, Marbach P, Petcher TJ. SMS 201-995: a very potent and selective octapeptide analogue of somatostatin with prolonged action. *Life Sci.* 1982; **31**: 1133–1140.
5. Cai RZ, Szoke B, Lu R, Fu D, Redding TW, Schally AV. Synthesis and biological activity of highly potent octapeptide analogs of somatostatin. *Proc. Natl. Acad. Sci. USA* 1986; **83**: 1896–1900.
6. Lamberts SW, van der Lely AJ, de Herder WW, Hofland LJ. Octreotide. *New Engl. J. Med.* 1996; **334**, 246–254.
7. Schally AV. Oncological applications of somatostatin analogues. *Cancer Res.* 1988; **48**: 6977–6985.
8. Logothetis CJ, Hossan EA, Smith TL. SMS 201-995 in the treatment of refractory prostatic carcinoma. *Anticancer Res.* 1994; **14**: 2731–2734.
9. Keri G, Mezo I, Horvath A, Vadasz Z, Balogh A, Idei M, Vantus T, Teplan I, Mak M, Horvath J *et al.* Novel somatostatin analogs with tyrosine kinase inhibitory and antitumor activity. *Biochem. Biophys. Res. Commun.* 1993; **191**: 681–687.
10. Keri G, Mezo I, Vadasz Z, Horvath A, Idei M, Vantus T, Balogh A, Bokonyi G, Bajor T, Teplan I *et al.* Structure–activity relationship studies of novel somatostatin analogs with antitumor activity. *Peptide Res.* 1993; **6**: 281–288.
11. Keri G, Erchegyi J, Horvath A, Mezo I, Idei M, Vantus T, Balogh A, Vadasz Z, Bokonyi G, Seprodi J, Teplan I, O Csuka, Tejeda M, Gaal D, Szegedi Z, Szende B, Roze C, Kalthoff H, Ullrich A. A tumor-selective somatostatin analog (TT-232) with strong *in vitro* and *in vivo* antitumor activity. *Proc. Natl. Acad. Sci. USA* 1996; **93**: 12513–12518.
12. Jaspers H, Horvath A, Mezo I, Keri G, Vanbinst G. Conformational study of a series of somatostatin analogues with antitumor and/or GH inhibitory activity. *Int. J. Peptide Prot. Res.* 1994; **43**: 271–276.
13. Fan CX, Hao XL, Ye YH. A novel organophosphorus compound as a coupling reagent for peptide synthesis. *Synth. Commun.* 1996; **26**: 1455–1460.
14. Zheng H, Fink D, Li H, Jiang X, Aebi S, Law P, Goodman M, Howell S. *In vitro* antineoplastic activity of a novel lanthionine-containing peptide. *Clinic Cancer Res.* 1997; **3**: 1323–1330.
15. Raynor K, Murphy WA, Coy DH, Taylor JE, Moreau JP, Yasuda K, Bell GI, Reisine T. Cloned somatostatin receptors: identification of subtype-selective peptides and demonstration of high affinity binding of linear peptides. *Mol. Pharmacol.* 1993; **43**: 838–844.
16. Raynor K, O'Carroll AM, Kong H, Yasuda K, Mahan LC, Bell GI, Reisine T. Characterization of cloned somatostatin receptors SSTR4 and SSTR5. *Mol. Pharmacol.* 1993; **44**: 385–392.
17. Jung G. *Lantibiotics*. Leiden: ESCOM, 1991; 1–34.
18. Osapay G, Prokai L, Kim HS, Medzihradszky KF, Coy DH, Liapakis G, Reisine T, Melacini G, Zhu Q, Wang SH, Mattern RH, Goodman M. Lanthionine–somatostatin analogs: synthesis, characterization, biological activity, and enzymatic stability studies. *J. Med. Chem.* 1997; **40**: 2241–2251.
19. Shao H, Wang SHH, Lee CW, Osapay G, Goodman M. A facile synthesis of orthogonally protected stereoisomeric lanthionines by regioselective ring opening of serine beta-lactone derivatives. *J. Org. Chem.* 1995; **60**: 2956–2957.

